




Please cite the Published Version

Salah ud din, M , Ur Rehman, MA , Ullah, R, Park, CW, Kim, DH and Kim, BS  (2022) Improving resource-constrained IoT device lifetimes by mitigating redundant transmissions across heterogeneous wireless multimedia of things. *Digital Communications and Networks*, 8 (5). pp. 778-790. ISSN 2468-5925

DOI: <https://doi.org/10.1016/j.dcan.2021.09.004>

Publisher: Elsevier BV

Version: Published Version

Downloaded from: <https://e-space.mmu.ac.uk/636416/>

Usage rights:  [Creative Commons: Attribution-Noncommercial-No Derivative Works 4.0](https://creativecommons.org/licenses/by-nc-nd/4.0/)

Additional Information: This is an open access article which first appeared in *Digital Communications and Networks*

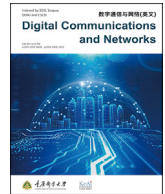
Enquiries:

If you have questions about this document, contact openresearch@mmu.ac.uk. Please include the URL of the record in e-space. If you believe that your, or a third party's rights have been compromised through this document please see our Take Down policy (available from <https://www.mmu.ac.uk/library/using-the-library/policies-and-guidelines>)



Contents lists available at ScienceDirect

Digital Communications and Networks

journal homepage: www.keaipublishing.com/dcan

Improving resource-constrained IoT device lifetimes by mitigating redundant transmissions across heterogeneous wireless multimedia of things



Muhammad Salah ud din^a, Muhammad Atif Ur Rehman^b, Rehmat Ullah^c, Chan-Won Park^d, Dae Ho Kim^d, Byung-seo Kim^{e,*}

^a Department of Electronics & Computer Engineering, Hongik University, Sejong City, 30016, South Korea

^b Department of Computing & Mathematics Manchester Metropolitan University, United Kingdom

^c Cardiff School of Technologies, Cardiff Metropolitan University, Cardiff, CF5 2YB, United Kingdom

^d Electronics and Telecommunications Research Institute, Daejeon, 34129, South Korea

^e Department of Software and Communications Engineering, Hongik University, Sejong City, 30016, South Korea

ARTICLE INFO

Keywords:

Clustering
WMSN
WSN
IoT's
Resource-constrained
Fuzzy
AHP
Sub clustering
MAC
Energy efficiency
Network lifetime

ABSTRACT

In Wireless Multimedia Sensor Networks (WMSNs), nodes capable of retrieving video, audio, images, and small scale sensor data, tend to generate immense traffic of various types. The energy-efficient transmission of such a vast amount of heterogeneous multimedia content while simultaneously ensuring the quality of service and optimal energy consumption is indispensable. Therefore, we propose a Power-Efficient Wireless Multimedia of Things (PE-WMoT), a robust and energy-efficient cluster-based mechanism to improve the overall lifetime of WMSNs. In a PE-WMoT, nodes declare themselves Cluster Heads (CHs) based on available resources. Once cluster formation and CH declaration processes are completed, the Sub-Cluster (SC) formation process triggers, in which application base nodes within close vicinity of each other organize themselves under the administration of a Sub-Cluster Head (SCH). The SCH gathers data from member nodes, removes redundancies, and forwards miniaturized data to its respective CH. PE-WMoT adopts a fuzzy-based technique named the analytical hierarchical process, which enables CHs to select an optimal SCH among available SCs. A PE-WMoT also devises a robust scheduling mechanism between CH, SCH, and child nodes to enable collision-free data transmission. Simulation results revealed that a PE-WMoT significantly reduces the number of redundant packet transmissions, improves energy consumption of the network, and effectively increases network throughput.

1. Introduction

Recently Wireless Multimedia Sensor Networks (WMSNs) have got huge attention from academia and industry. These networks have been widely adopted in various application fields, such as smart agriculture [1], battlefield surveillance [2–5], habitat monitoring [6], environment monitoring [7], smart health care [8], smart buildings [9,10], and forest fire monitoring [11]. The deployed nodes in a WMSN are usually equipped with several multimedia modules (e.g., microphones and cameras). These modules enable the nodes to capture and transmit scalar as well as multimedia content in the form of still images, audio streams, and video streams. While a node may capture a snapshot of short-duration events, it may also capture multimedia streaming for

longer-duration events depending on the application's requirements [12].

In WMSNs, the productive utilization of energy, storage, and computational capability have significant importance to achieve an increased network lifetime. To optimize energy consumption, the network architecture plays a vital role in efficient resource utilization [13]. In this regard, several efforts have been devoted in the literature to developing an efficient network design. These proposed network compositions include 1) single-tier flat network architecture, 2) cluster-based architecture, and 3) multi-tier network architecture [14,15].

In *single-tier flat architecture*, the network is deployed with homogeneous sensor nodes of identical functionalities and available resource capabilities. In this architecture, each underlying network node may

* Corresponding author.

E-mail addresses: salah_udin@outlook.com (M. Salah ud din), atif_r@outlook.com (M.A. Ur Rehman), rullah@cardiffmet.ac.uk (R. Ullah), cwp@etri.re.kr (C.-W. Park), dhkim7256@etri.re.kr (D.H. Kim), jsnbs@hongik.ac.kr (B.-s. Kim).

<https://doi.org/10.1016/j.dcan.2021.09.004>

Received 21 December 2020; Received in revised form 7 September 2021; Accepted 7 September 2021

Available online 14 September 2021

2352-8648/© 2021 Chongqing University of Posts and Telecommunications. Publishing Services by Elsevier B.V. on behalf of KeAi Communications Co. Ltd. This is an

open access article under the CC BY-NC-ND license (<http://creativecommons.org/licenses/by-nc-nd/4.0/>).

perform any operation, ranging from sensing and visual data acquisition utilizing multimedia modules to data forwarding towards the sink node via single or multihops. In *cluster-based architecture*, the network is composed of heterogeneous sensing nodes (e.g., multimedia and scalar). These nodes organize themselves into groups named clusters. A leader node, referred as a Cluster Head (CH), is elected from various nodes located in the vicinity of each other to manage the cluster in terms of performing aggregation operations on data received from child nodes, data processing, and the data transmission towards the sink node. In such architecture, the CH often has more resources and performs compute-intensive tasks as mentioned above. The overall network energy consumption in cluster-based architecture is an order of magnitude less than the single-tier flat architecture networks. The reason is that the child nodes in cluster-based architecture forward data towards the relatively closely-positioned CH; hence, those nodes require low power transmissions, resulting in a low amount of energy consumption. The *multi-tier architecture* consists of various tiers where each tier may include both homogeneous and heterogeneous nodes. Typically, the first tier is comprised of scalar nodes performing various operations, including temperature sensing, motion detection, and vibration sensing. The second tier may consist of multimedia sensor nodes that may perform complex operations, including visual data acquisition, object detection, and recognition of acquired data. The third tier is composed of resource-rich nodes compared to the nodes in tier-1 and tier-2. These nodes usually perform compute-intensive tasks, such as applying deep learning models to extract features from acquired data, facilitating lower tier nodes to perform complex computations, and data forwarding towards the sink node [15].

Among the aforementioned network architectures, clustering is the most prominent mechanism for achieving energy efficiency in WMSNs. Clustering algorithms effectively enhance network lifetime, balance network load, minimize latency, and increase network connectivity. These algorithms split the entire network into multiple clusters of various sizes, as shown in Fig. 1. A single high resource node from each cluster is elected as CH, making it responsible for its cluster administration. The CH is positioned at a shorter distance from its child nodes. Therefore, child nodes forward their sensed data to their corresponding CH instead of performing a direct transmission to the sink node (usually located at a farther distance). This results in improved utilization of network resources (e.g., residual energy) [16].

After data collection, a CH aggregates the data, removes redundancies from the aggregated data, and transmits it to the sink node. As a CH manages its whole cluster (in terms of data collection, aggregation, and transmission as well as transmission scheduling), a CH consume more

energy than a child node. Therefore, an efficient CH selection mechanism can play a prominent role in increasing the overall network's operation period.

In conventional cluster-based schemes for WMSNs, the CH assigns a Time Division Multiple Access (TDMA) slot to each child node in its cluster for performing data transmission [17]. However, similar types of nodes (e.g., audio, video, and scalar) may be nearby, causing them to capture identical data that gets forwarded to the CH. This unnecessary data transmission may result in wasted resources, such as residual energy and storage. Since residual energy is of extreme importance [15], unnecessary data transmissions may diminish the available energy reservoir and prevent nodes from participating in network operations for a longer duration. Furthermore, a CH may not accommodate all the data from its members due to buffer constraints and increased processing time. This may induce network congestion, increased delays, and packet re-transmission. Therefore, the design of an energy-efficient mechanism is critical to enhancing network lifetime while satisfying the requisite Quality of Service (QoS) requirements of multimedia applications.

To address the aforementioned challenges, we propose a Power-efficient Wireless Multimedia of Things (PE-WMoT) protocol, an energy-efficient clustering scheme for heterogeneous WMSNs. The main contributions of the proposed scheme can be summarized as follows:

1. The PE-WMoT protocol provides a robust resource-aware clustering mechanism to curtail node energy consumption by enabling high resource nodes to declare themselves CHs.
2. The PE-WMoT protocol presents an efficient sub-clustering mechanism to further minimize unwanted data transmissions towards the main CH.
3. The PE-WMoT protocol designs an efficient slot scheduling mechanism to ensure collision-free data transmissions between child nodes, Sub-Cluster Heads (SCHs), and the CH.
4. Simulations are performed in Castalia (based on OMNET++) to reveal the performance of the PE-WMoT protocol with relevant and state-of-the-art schemes in terms of energy efficiency, packet delivery ratio, CH lifetime, and control overhead.

The rest of the paper is organized as follows. Section 2 is devoted to related work, Section 3 introduces the motivations and a detailed description of PE-WMoT protocol, Section 4 presents PE-WMoT data transmissions and collection at SCHs, performance evaluations are presented in Section 5, and finally, Section 6 draws the conclusion.

2. Related work

A myriad of energy-efficient schemes have been proposed for WMSNs to improve energy optimization for multimedia sensor nodes, enhancing overall network lifetime and QoS [18,19]. In this section, we review existing state-of-the-art energy-efficient schemes proposed for WMSNs.

To optimize energy consumption and enhance node lifetime in WMSNs, a pair-wise directional geographical routing was proposed [20]. A multipath routing scheme called “direct diffusion” [21] was also proposed that allowed each node to broadcast packets within its transmission range. Receiving nodes maintained sending node information, so when events occurred in the vicinity of any given node, the scheme could choose the best path for delivering the information to the managing node.

A Reliable Energy-Aware Routing (REAR) protocol for Wireless Sensor Networks (WSNs) [22] was proposed to address energy efficiency and reliable data delivery issues. In their work, the sink node broadcasted the service query packet in the network. Receiving nodes informed the sink node about their discovered path by forwarding the reservation message. However, REAR protocol performance could degrade in densely deployed networks since nodes may spend a large amount of time and consume significant energy in their path discovery processes. Ant-based Service-Aware Routing (ASAR) algorithm for WMSNs was presented in Ref. [23]. ASAR mainly focuses on routing between CHs and the sink node, in which the CH node forwards various classes of data to the sink

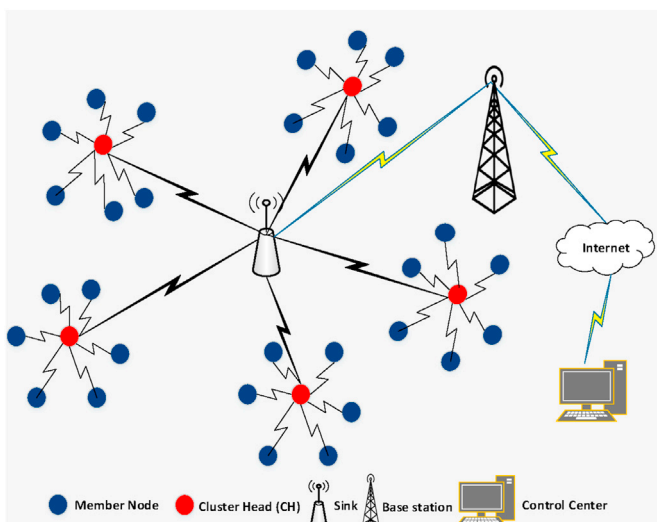


Fig. 1. Architecture of cluster-based WSNs.

node.

Another protocol, named “Low-energy Image Compression Algorithm (LEICA)” [24], for WMSNs proposed compressing visual data while maintaining the image quality. The results showed that the LEICA prolonged network lifetime by decreasing the energy consumed in transmission and computation. Additionally, an energy-efficient image compressive transmission scheme was proposed in Ref. [25]. The authors introduced the background subtraction of an image and blocked compressive sending to reduce energy consumption. In Ref. [26], a Lifetime Priority-Driven Resource Allocation (LP-DRA) was proposed for a Wireless Network Virtualization (WNV)-based Internet of things. LP-DRA assigns the available resources to Virtual Network Requests (VNRs) based on VNR lifetime and physical network revenue. LP-DRA ensured the effective utilization of physical resources, boosted the VNR acceptance rate, and effectively enhanced network revenue.

Efficient and accurate object classification in WMSNs was proposed in Ref. [27]. The classification utilized a genetic algorithm-based classifier with two simple characteristics from objects in audiovisual frames. Simulation with three object classes (animals, vehicles, and humans) produced a purported high level of accuracy without significant node storage overhead or energy consumption [26]. A multi-objective approach to solving WMSN routing problems was proposed in Ref. [28]. The authors considered naming delay and expected transmission counts in the QoS requirements. Their proposed mechanism improved energy optimization and delays.

To reduce energy consumption, the authors of [29] presented a clustering mechanism based on Heterogeneous WSNs Using Mixed-Integer Programming (HRMIP). In HRMIP, sensor nodes have a shorter average path that reduces total energy consumption. However, once the nodes are deployed, the path taken by the nodes to transmit data always remains fixed. Sensor nodes with high transmission rates may continue to consume large amounts of energy, with the potential for rapid death that lowers overall network lifetime.

3. Power-efficient wireless multimedia of things (PE-WMoT) protocol

In this section, we provide the motivation for our proposal, as well as some of its network assumptions, to illustrate PE-WMoT features. After that, a detailed explanation is provided.

3.1. PE-WMoT—Motivation

The motivation behind the PE-WMoT is illustrated by the use case scenario of battlefield surveillance, as depicted in Fig. 2. The figure depicts a heterogeneous WMSN comprised of several heterogeneous nodes randomly deployed in a region of interest to monitor intruders (e.g., enemy troops, warheads, armored cars, and tanks). These deployed nodes are divided into clusters, and a single node among each cluster performs CH duties. When an intrusion occurs, the underlying nodes capture the intruder and forward it to their respective CH.

Assuming enemy troops attack this critical zone, deployed nodes will capture troops activity and transmit it to their CH. It is highly likely that several identical application base nodes may reside in close proximity to one another, capture identical data and transmit it; this can overload the CH, increase the packet drop rate, and trigger network retransmissions.

In most cluster-based energy-efficient schemes [17,30], nodes positioned in an affected area forward their sensed data to their respective CH without considering neighboring nodes. They transmit identical data that highly degrades CH lifetime and can increase network congestion. Besides, some existing techniques [31] split the main cluster into subgroups based on overlapping Fields of Views (FoVs). These approaches allow only a single high energy node from each sub-group to forward data to the main CH in order to reduce the unnecessary transmissions. However, the designated high energy node may likely fail to transmit the data due to unforeseeable reasons (e.g., sudden hardware/software failure). A low

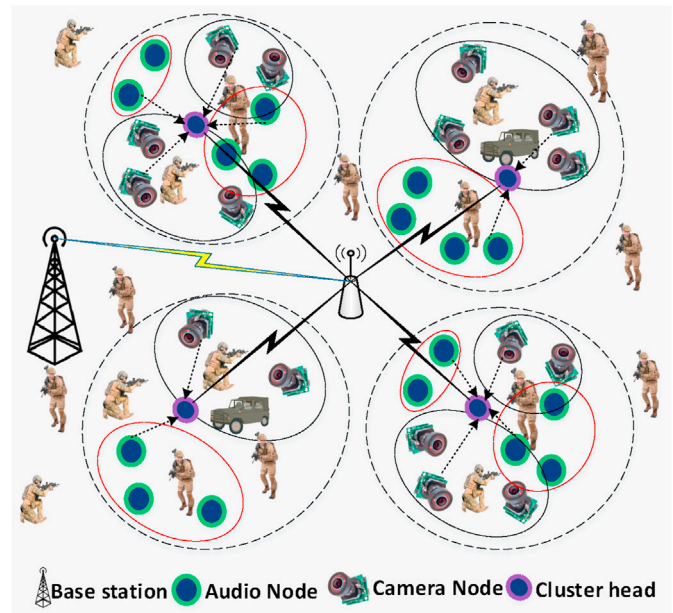


Fig. 2. Battlefield surveillance system.

energy node in a cluster may capture an event that requires timely action; however, due to its energy constraint, it cannot take part in data transmission. As in mission-critical applications (apart from energy optimization), data delivery is extremely important. The aforementioned schemes may affect application performance and QoS by way of data loss.

The main objective of the PE-WMoT protocol is to put forward a robust mechanism that mitigates redundant transmissions, minimizes node energy consumption, and enhances the network operation time while ensuring sensed data integrity.

3.2. PE-WMoT—Network assumptions

We consider a WMSN where several heterogeneous multimedia sensor nodes are sprinkled randomly in the sensing region. The concept of heterogeneity is defined in terms of available resources (e.g., residual energy, storage, and computational capability) and node type (e.g., multimedia, scalar). We assume that all nodes are static and each node is equipped with a digital compass (for estimating camera direction) and a GPS module (for acquiring its geographic location) [32].

3.3. PE-WMoT protocol description

The PE-WMoT protocol comprises various phases (e.g., cluster formation, CH declaration, SC formation, and neighbor information sharing phases), neighbor information sharing to the main CH, SCH election, and the data transmission and data collection at the SCH. The protocol deploys several heterogeneous WSNs nodes randomly deployed in the region of interest. These nodes are organized into clusters with one CH node among each cluster. Each cluster is further divided into SCs, as shown in Fig. 3.

A single high energy node from each SC shares its member information with the CH. After accumulating the information, the CH applies the Analytical Hierarchy Process (AHP) to elect the potential SCH in each SC. SCH selection is based on a multitude of available parameters, such as residual energy, available storage, physical location, and computational capability.

Upon SCH election, the CH disseminates the elected SCH information (i.e., SCH list) along with the TDMA slots for each SCH node. On receiving the SCH list, each node searches for its node-ID on the list. If a node finds its node-ID, it considers itself SCH, divides the allocated

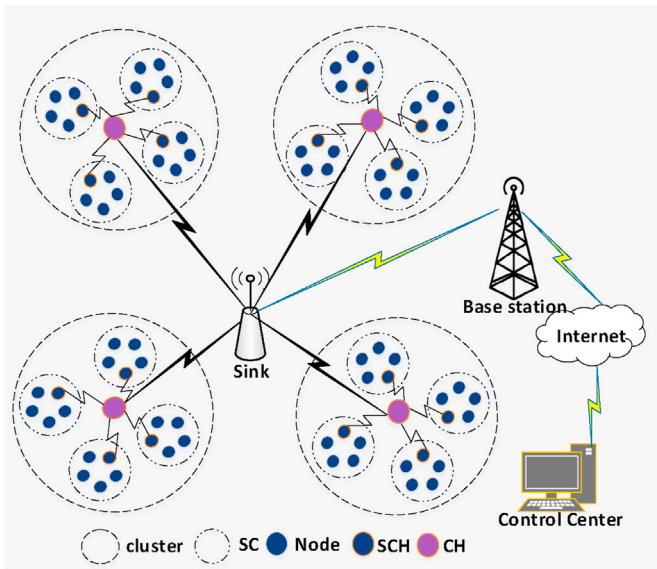


Fig. 3. PE-WMoT: Sub-clustering architecture.

TDMA slot into mini slots (as per the number of child nodes in the SC), and assigns them to each SC member node. Each node in the SC transmits the sensed data to the SCH in its allocated mini slot. Finally, the SCH forwards the aggregated data to the main CH node. In a PE-WMoT, the control packet transmissions (e.g., HELLO, CH advertisement, and neighbor association) follow a contention-based mechanism—Carrier-sense Multiple Access with Collision Avoidance (CSMA/CA), while the data transmissions (i.e., between member nodes and S-CH, between S-CH and CH) are based on TDMA.

The complete frame structure and slot assignments are presented in Fig. 4, and a comprehensive description of all phases is presented in the following subsections.

3.3.1. PE-WMoT cluster formation and CH declaration phase

The cluster formation and CH declaration process is based on our previous work [3], where nodes with available resources greater than a certain application-specific threshold are eligible to participate in the CH declaration process.

3.3.2. PE-WMoT—Subcluster formation and neighbor information sharing

The subclustering mechanism triggers soon after the completion of CH declaration process. Each node broadcasts a Hello message in its transmission radius composed of a message type (i.e., Hello message), Source Media Access Control (SRC-MAC) address, node type (e.g., multimedia, scalar), Cluster Head Media Access Control (CH-MAC) address, location (e.g., X and Y node coordinates), Residual Energy (RES-E) of the node, and directional FoV information. The Hello message format is shown in Fig. 5 and summarized as follows.

- Packet type: The packet type field represents the type of packet (e.g., Hello message). The packet type will be set as described in Table 1.
- SRC-MAC address: The SRC-MAC address field is the 16-bit MAC address of the node that uniquely identifies the originator node.
- Node-type: The node-type two-bit specifies the type of node (e.g., scalar or multimedia). The value 00 represents the scalar node, whereas the value 01 represents a multimedia node. The remaining values (i.e., 10 and 11) are reserved for future use.
- CH-MAC address: The CH-MAC address field is the 16-bit MAC address of the CH node.
- Res-E: The Res-E is a 16-bit field that specifies a node's residual energy.
- LOC: The LOC field is the 16-bit geographic location (i.e., X- and Y-coordinates) of the node.
- FoV: The FoV is a 9-bit field that represents the directional view of a multimedia sensor node. FoV is supposed to be an isosceles triangle with a vertex angle θ and whose congruent sides length depicts the sensing range R_s and orientation α . The sensor is deployed at a position L with respective location coordinates $X_l Y_l$ [33].

On receiving the Hello message, each node (under the administration of an identical CH) computes its neighbor table based on its node type and location. By doing so, identical application type nodes in close proximity organize themselves in SC.

3.3.3. PE-WMoT: neighbor information sharing to main CH

In existing schemes [17,29], each node in the network forwards the Join-CH-message to associate itself with the CH. The transmission of association messages from each node produces additional overhead in the network. To reduce this overhead, only a single high energy node

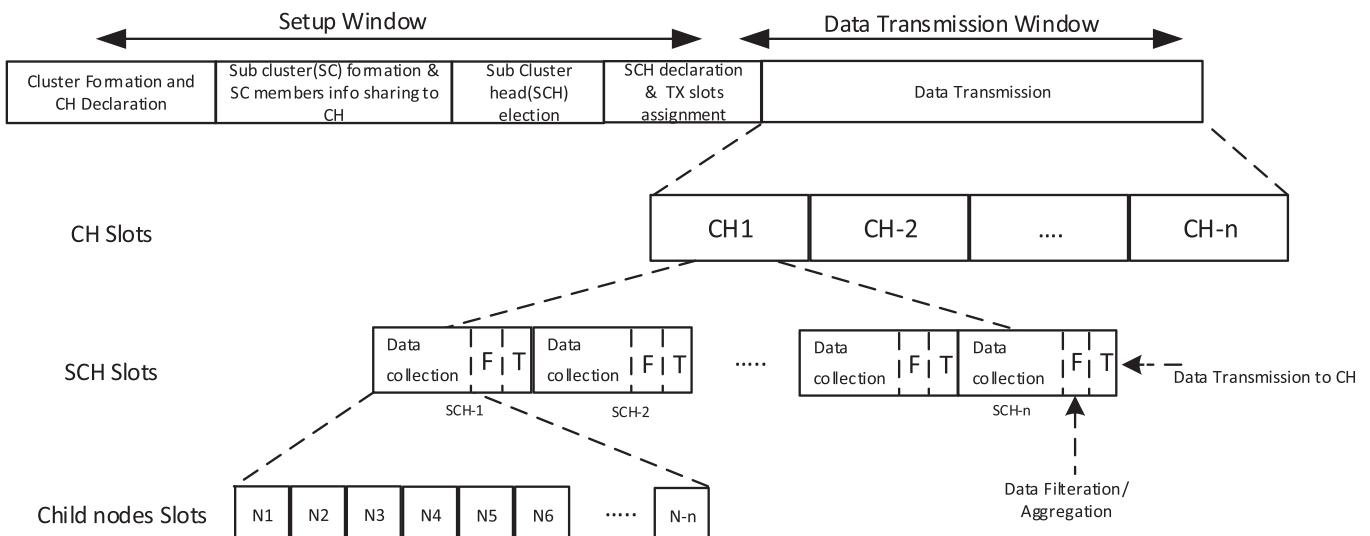


Fig. 4. PE-WMoT: Time slots management.

Packet Type	Src-MAC address	Node-Type	CH-MAC address	Res-E	Loc	FoV
Size(bits)	3	16	2	16	16	9

Fig. 5. PE-WMoT: HELLO message format.

from each SC shares its members' information with the CH by forwarding the *NgbrINFO* message towards the main CH node. The *NgbrINFO* packet is composed of the packet type, SRC-MAC address, CH-MAC address, and members' information list (see Fig. 6) is summarized as follows.

Packet Type	SRC-MAC address	CH-MAC address	Members Info list	
Size(bits)	3	16	16	Variable

Fig. 6. PE-WMoT: neighbor information packet structure.

- Packet type: The packet type field represents the type of packet. The value 010 represents the *NgbrINFO* packet, as discussed in Table 1.
- SRC-MAC address: The SRC-MAC address field is the 16-bit MAC address of the source node.
- CH-MAC address: The CH-MAC address field is the 16-bit MAC address of the CH node.
- Members' info list: The members' info list contains the information of neighboring nodes. It is comprised of the node's available resources, and its size depends on the number of nodes present in the neighbor table.

3.3.4. PE-WMoT—SCH election

A CH may receive multiple *NgbrINFO* messages from its neighbors' SCs. Upon receiving the *NgbrINFO* packets, the CH employs the AHP to select a potential SCH in each SC. Since the nodes are heterogeneous, the CH must select an SCH node with maximum available resources. The rationale is that the SCH requires high resources to perform data aggregation and filtration, data collection, and data transmission to the main CH. By adopting the AHP, the CH selects the optimal SCH among several potential SCH candidates. Once SCH election finalizes, the CH assigns the transmission schedule for each elected SCH by advertising the SCH-TX packet. The SCH-TX packet structure is shown in Fig. 7 and defined as follows.

Packet Type	CH-MAC address	SCH-list	TX-schedule	
Size(bits)	3	16	Variable	Variable

Fig. 7. PE-WMoT: SCH-TX packet.

- Packet type: The packet type field represents the type of packet. The value 011 represents the packet, as discussed in Table 1.
- CH-MAC address: The CH-MAC address field represents the 16-bit MAC address of the CH node.
- SCH-list: The SCH-list contains elected SCH nodes. The size of the list depends on the number of SCH nodes.
- TX-schedule: The TX-schedule field specifies the time allocated by the CH node to each SCH for data transmission.

Each child node in the cluster may receive the SCH-TX message and inquire whether its node-ID exists in the message. If the node finds its node-ID, the node becomes an SCH. The selected SCH divides its assigned time slot into equalized mini time-slots for the following purposes: 1) child node data transmission towards the SCH, 2) data filtration to remove redundancies in the aggregated data, and 3) forwarding slot to forward aggregated data to the main CH.

A step-wise detailed description of the SCH election process adopting

the AHP [34] is expressed as follows.

1. Structuring hierarchy:

The main goal (i.e., the selection of the optimal SCH in each SC) is placed at the uppermost hierarchy level, as shown in Fig. 8. The next hierarchy level is comprised of the decision factors. The lowest level contains all the candidate nodes that need to be determined.

2. Compute the local-weight vector and consistency check:

The technique for determining the local weight (i.e., weight of each decision factor) is illustrated as follows.

(a) Pairwise comparison development:

$$A1 = \begin{pmatrix} a_{11} & a_{12} & a_{13} & \dots & a_{1n} \\ a_{21} & a_{22} & a_{23} & \dots & a_{2n} \\ a_{31} & a_{32} & a_{33} & \dots & a_{3n} \\ \vdots & \vdots & \vdots & \ddots & \vdots \\ a_{n1} & a_{n2} & a_{n3} & \dots & a_{nn} \end{pmatrix}; a_{ij} = \frac{1}{a_{ji}} \quad (1)$$

To calculate the weights, AHP develops a decision matrix by employing a pairwise comparison of the decision factors, as shown in Eq. (1).

Consider matrix $A1 (n \times n)$, where n denotes the number of decision factors (e.g., the residual energy of the node, computational capability, available storage, and the distance of the node from the CH). Each entry in $A1$ (e.g., a_{ij}) indicates the significance of the i_{th} decision factor with respect to the j_{th} decision factor. If $a_{ij} > 1$, the i_{th} decision factor is more important than the j_{th} decision factor. However, if $a_{ij} < 1$, the i_{th} decision factor has less importance than the j_{th} decision factor. Moreover, $a_{ij} = 1$ depicts equal importance for the i_{th} and j_{th} decision factor indicates the rank of s . Each decision factor is decided as per the application's requirements based on Saaty's fundamental scale [34], as shown in Table 2.

(b) Weights computation:

The significance of each decision factor is computed by

$$W_k = \frac{\left(\prod_{j=1}^n a_{kj} \right)^{\frac{1}{n}}}{\sum_{i=1}^n \left(\prod_{j=1}^n a_{ij} \right)^{\frac{1}{n}}} \quad k = 1, 2, \dots, n \quad (2)$$

where W_k expresses the weight of the k_{th} decision factor. The weights computed from Eq. (2) are arranged in a matrix (i.e., W) and defined as follows:

(c) Compute the maximum eigenvalue (λ_{max}), consistency index (CI), and consistency ratio (CR):

$$W = \begin{pmatrix} W_1 \\ W_2 \\ W_3 \\ \vdots \\ W_n \end{pmatrix} \quad (3)$$

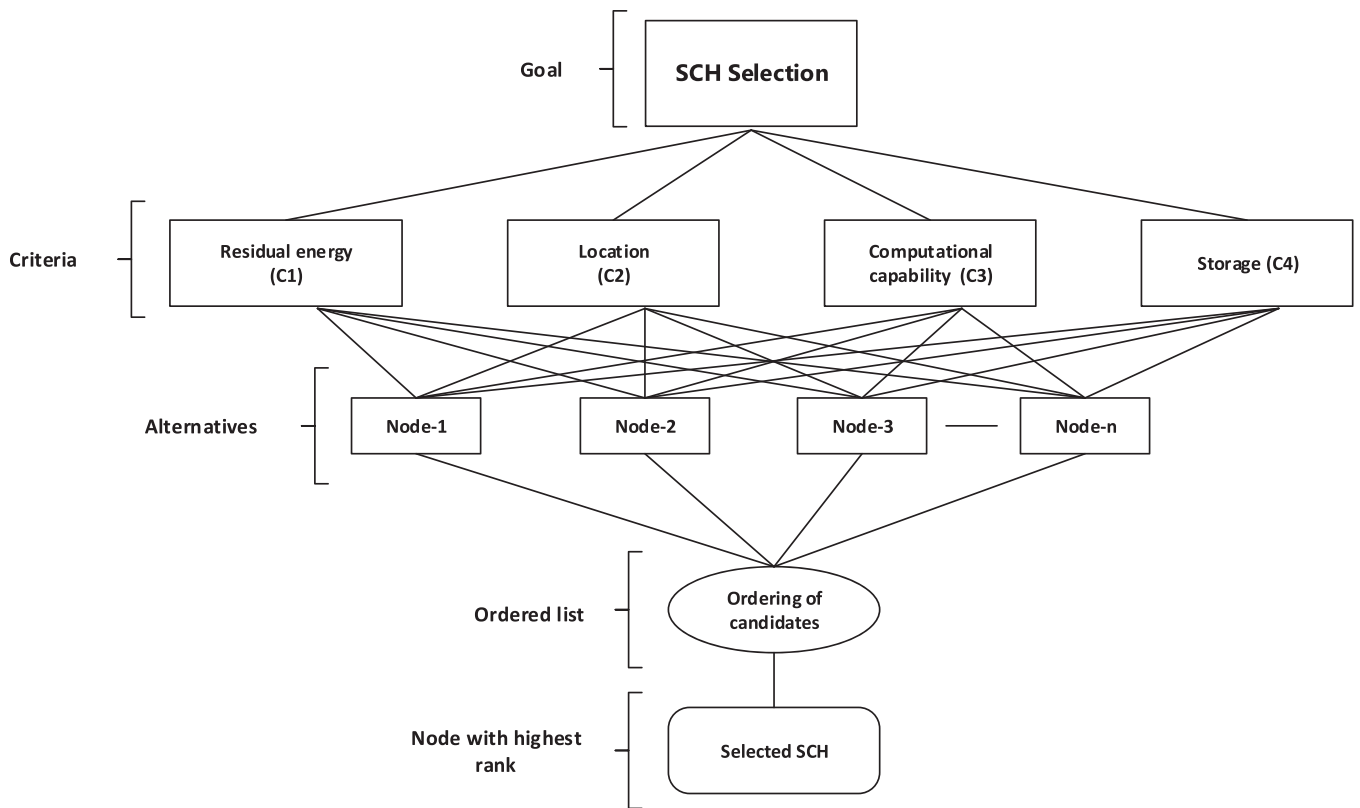


Fig. 8. AHP structure for SCH selection.

Table 1 Packet types and meanings.

Packet type	Description
000	CH announcement
001	HELLO message
010	Neighbor info
011	SCH-Transmission schedule
100	Node data packet
101	SCH data packet

Table 2 Saaty's Fundamental scale.

Importance level	Definition
1	Equally important
3	Moderately important
5	Strongly important
7	Very strongly important
9	Extremely important
2,4,6,8	Intermediate values

The eigenvalue (λ_{max}) of $A1$ is computed using Eq. (4).

$$A3 = \begin{pmatrix} a_{11} & a_{12} & a_{13} & a_{1n} \\ a_{21} & a_{22} & a_{23} & a_{2n} \\ a_{31} & a_{32} & a_{33} & a_{3n} \\ \cdot & \cdot & \cdot & \cdot \\ \cdot & \cdot & \cdot & \cdot \\ a_{n1} & a_{n2} & a_{n3} & a_{nn} \end{pmatrix} \times \begin{pmatrix} W_1 \\ W_2 \\ W_3 \\ \cdot \\ \cdot \\ W_n \end{pmatrix} \quad (4)$$

$$A3_i = \frac{(A1 \times W)_i}{W_i} \quad \text{where } i = 1, \dots, n \quad (5)$$

In Eq. (5), each element of the $A3$ (i.e., $n \times n$) matrix is divided by its corresponding W (i.e., $n \times 1$) matrix (i.e., element-by-element division).

The result computed from Eq. (5) is the $n \times 1$ matrix. The eigenvalue (λ_{max}) is computed by taking the average of the $A3$ matrix:

$$\lambda_{max} = \frac{\sum_{i=1}^n A3_i}{n} \quad (6)$$

where n is the total number of elements in the $A3$ matrix.

To check the consistency of matrix $A1$, we have to compute CR , which is defined as the ratio of the CI to the Random Index (RI):

$$CI = \frac{\lambda_{max} - n}{n - 1} \quad (7)$$

$$CR = \frac{CI}{RI} \quad (8)$$

where RI can be selected as per the number of decision factors. For instance, if there are three decision factors, the corresponding RI value will be 0.58, as shown in Table 3.

If $0 \leq CR < 0.1$, the computed weights (e.g., W in Eq. (3)) are consistent; otherwise, the weights are not reliable and need to be recalculated, which requires the reconsideration of all criteria significance to

Table 3 Saaty's RI table.

Decision factors	Value
2	0
3	0.58
4	0.9
5	1.12
6	1.24
7	1.32
8	1.41
9	1.45
10	1.51

achieve the consistency check constraint (i.e., $0 \leq CR < 0.1$).

3. Decision matrix development:

An SC is comprised of an m number of nodes. The CH organizes the SC nodes and their attributes (e.g., decision factors) in a tabular form, defined in Table 4.

Table 4
SC nodes and decision factors.

	C_1	C_2	C_3	.	.	C_n
N_1	$V_{1,1}$	$V_{1,2}$	$V_{1,3}$.	.	$V_{1,n}$
N_2	$V_{2,1}$	$V_{2,2}$	$V_{2,3}$.	.	$V_{2,n}$
N_3	$V_{3,1}$	$V_{3,2}$	$V_{3,3}$.	.	$V_{3,n}$
.
.
N_m	$V_{m,1}$	$V_{m,2}$	$V_{m,3}$.	.	$V_{m,n}$

(d) Model synthesis and final decision: The weights computed for each decision criterion by employing the AHP:

$$\begin{pmatrix} C_1 \\ C_2 \\ C_3 \\ \vdots \\ C_n \end{pmatrix} = \begin{pmatrix} W_1 \\ W_2 \\ W_3 \\ \vdots \\ W_n \end{pmatrix} \tag{9}$$

In Table 4, N represents the SC member node, $V_{m,n}$ denotes the value of the n th decision factor of the m th node, m is the total number of nodes in an SC, and n is the number of decision factors.

4. Decision factor scaling:

Since the decision factor values do not lie in the same range, they need to be tuned to a common range (e.g., [0 1]). The scaled form of the decision factors is computed as follows:

$$V^*_{(i,j)} = \frac{V_{(i,j)}}{\sqrt{\sum_{k=1}^m V^2_{(k,j)}}} \text{ where } i = 1..m \text{ and } j = 1..n \tag{10}$$

The scaled decision factor values of all nodes are shown in Table 5.

Table 5
Scaled decision factors.

	C_1	C_2	C_3	C_n
N_1	$V^*_{1,1}$	$V^*_{1,2}$	$V^*_{1,3}$	$V^*_{1,n}$
N_2	$V^*_{2,1}$	$V^*_{2,2}$	$V^*_{2,3}$	$V^*_{2,n}$
N_3	$V^*_{3,1}$	$V^*_{3,2}$	$V^*_{3,3}$	$V^*_{3,n}$
N_m	$V^*_{m,1}$	$V^*_{m,2}$	$V^*_{m,3}$	$V^*_{m,n}$

5. Rank assignment and SCH selection:

The allocated weights and corresponding criteria are shown in Table 6. The rank of each child node in the SC is derived by employing Eq. (11) and depicted in Table 6.

Once the R of each child node of the SC is computed, the main CH organizes the child nodes in increasing order by priority (e.g., R_1, R_2, \dots, R_n). The detailed mechanism of SCH election is depicted in Algorithm 1.

Algorithm 1 SCH(s) Election

```

1: procedure SCH(s) ELECTION
2: memsList ← list of identical nodes
3: i ← ith decision factor
4: j ← jth decision factor
5: numDecFacts ← total decision factors
6: Compute comparison matrix (A1) by Eq. 1;
7: for k ← 1 to numDecFacts do
8:   Compute the weights decision factors i.e.,

```

$$W_k = \frac{\left(\prod_{j=1}^n a_{kj}\right)^{\frac{1}{n}}}{\sum_{i=1}^n \left(\prod_{j=1}^n a_{ij}\right)^{\frac{1}{n}}}, \quad k = 1, 2, 3, \dots, n$$

```

9: end for
10: Insert computed weights in matrix(W) by Eq.3
11: Compute A3 matrix by employing Eq. 5
12: Element by element division of A3 and W i.e.,
13: for i ← 1 to numDecFacts do

```

$$A3_i = \frac{(A1 \times W)_i}{W_i}, \text{ where } i = 1, \dots, n$$

```

14: end for
15: Compute the eigenvalue  $\lambda_{max}$  i.e.,

```

$$\lambda_{max} = \frac{\sum_{i=1}^n A3_i}{n}$$

```

16: Compute the consistency index CI i.e.,

```

$$CI = \frac{\lambda_{max} - n}{n - 1}$$

```

17: Compute the Consistency ratio i.e.,

```

$$CR = \frac{CI}{RI}$$

```

18: verify the CR i.e., !(0 ≤ CR < 0.1) re-compute weights
19: if (memsList.length > 1) then
20:   for i ← 1 to sizeOfmemsList do
21:     Get member nodes from memsList
22:     Insert nodes attributes in a table
23:     Normalize the values of attributes i.e.,

```

$$V^*_{(i,j)} = \frac{V_{(i,j)}}{\sqrt{\sum_{k=1}^m V^2_{(k,j)}}} \text{ where } i = 1..m \text{ and } j = 1..n$$

```

24:     Insert normalized values in table
25:     Assign weights to each attribute i.e.,

```

$$N_{i,j} = w_j \times V^*_{i,j} \text{ where } i = 1..m, j = 1..n$$

```

26:     Compute the rank of each node i.e.,

```

$$R_i = \sum_{j=1}^n (W_j \times V^*_{i,j}) \text{ where } i = 1..m,$$

```

27:     Insert rank in rankList
28:   end for
29: end if
30: Search the node with highest rank in rankList
31: Declare the highest rank node as SCH
32: end procedure

```

4. PE-WMoT—data transmission and collection at the SCH

PE-WMoT protocol provides two data transmission mechanisms: 1) sensor node data transmission, and 2) SCH data transmission. In the former, sensor nodes transmit their sensed data to their respective SCH in

Table 6
Child nodes Ranks.

	C_1	C_2	C_n
N_1	$W_1 \times V_{1,1}^*$	$W_2 \times V_{1,2}^*$	$W_n \times V_{1,n}^*$
N_2	$W_1 \times V_{2,1}^*$	$W_2 \times V_{2,2}^*$	$W_n \times V_{2,n}^*$
N_3	$W_1 \times V_{3,1}^*$	$W_2 \times V_{3,2}^*$	$W_n \times V_{3,n}^*$
N_m	$W_1 \times V_{m,1}^*$	$W_2 \times V_{m,2}^*$	$W_n \times V_{m,n}^*$

$$R_i = \sum_{j=1}^n (W_j \times V_{i,j}) \quad \text{where } i = 1..m, \quad (11)$$

where R indicates the rank of the child node. their corresponding time slot, whereas the latter is utilized by the SCH to transmit its processed data to the main CH.

The following subsections provide detailed descriptions for each mechanism.

4.1. PE-WMoT — sensor node data transmission

After sensing the environment, each node waits for its allocated time slot. When this slot begins, each node transmits its captured data to its respective SCH. The packet format of a child node is illustrated in Fig. 9.

	Packet Type	SRC-MAC address	SCH-MAC address	Payload
Size(bits)	3	16	16	Variable

Fig. 9. PE-WMoT: Child node data packet format.

- Packet type: The packet type field represents the type of packet. The value 100 represents the child node data packet, as discussed in Table 1.
- The SRC-MAC address field is the 16-bit MAC address of the originator node.
- SCH-MAC address: The SCH-MAC address field is the 16-bit MAC address of the SCH node.
- Payload: The payload field has a variable length and is composed of the data sensed by the child node.

4.2. PE-WMoT — SCH data transmission

The SCH aggregates the data received from its subordinates (child nodes) and forwards it to the main CH. The data packet format of the SCH node is shown in Fig. 10.

	Packet Type	SRC-MAC address	CH-MAC address	RES-E	Aggregated Data
Size(bits)	3	16	16	16	Variable

Fig. 10. PE-WMoT: SCH Data packet format.

- Packet type: The packet type field represents the type of packet. The value 101 represents the SCH data packet, as discussed in Table 1.
- SRC-MAC address: The SRC-MAC address field is the 16-bit MAC address of the SCH node.
- CH-MAC address: The CH-MAC address field is the 16-bit MAC address of the main CH node.
- RES-E: The RES-E field specifies the residual energy information of the SCH node.
- Aggregated data: The aggregated data field has a variable length and contains data aggregated from the child nodes. The size of the aggregated data field depends on the number of nodes in the SC.

4.3. PE-WMoT—data collection use case scenarios

As discussed, multimedia nodes may have a directional FoV. These nodes capture intrusions that happen within their observation region (i.e., FoV). The transmission of intruder information captured by multiple (closely located) sensor nodes towards the main CH not only affects CH lifetime, but also reduces child node residual energy.

To optimize child and CH node energy consumption, the PE-WMoT protocol enables child nodes to forward their data to their respective SCH while each SCH filters data received from its subordinates and minimizes the number of unessential transmissions in the network. To this end, PE-WMoT incorporates the various traffic generation patterns in terms of traffic generation rate based on directional FoVs, and discussed as follows.

- a. **Nodes with different FoVs facing the same direction:** These nodes are depicted in Fig. 11(a), facing the same direction but with observations that can differ due to FoV. Considering only the direction faced and allocating a single high-resource node to forward information can cause data loss and affect application QoS, as captured data might not be forwarded due to low resource availability. The use case scenario of this type of deployment is as follows:

Consider three multimedia nodes M1, M2, and M3 (Fig. 11(a)) pointing in the same direction while possessing different FoVs. When a mobile object (intruder) moves through the FoV of any node, the node will be activated and capture the intruder's movement. Captured data may differ between nodes due to differing FoVs. M1 captures the intruder without a weapon in its hand. However, when the intruder moves in the vicinity of M2, the captured image shows the intruder has some weapon in its hand. Contrast this with M3 capturing the intruder during shooting. Due to close deployment and matching application type, if only the high-resource node transmits to the main CH, the captured data may degrade the application QoS since the object may not be captured accurately by the nominated node. However, in PE-WMoT, all child nodes in an SC transfer their sensed data to the SCH in their respective time slots to conserve the captured data integrity.

- b. **Nodes with matching FoVs that face different directions:** These nodes are depicted in Fig. 11(b). As all nodes have the same FoV, they may capture similar data despite facing different directions. This may result in unnecessary data transmissions and waste resources. The use case of the above-mentioned deployment is as follows:

In security surveillance applications, the primary objective is to detect and track the objects that attempt to approach sensitive areas (e.g., the camp or site). When an object moves towards the sensitive region, the intrusion may be tracked by several sensing nodes. The transmission of the sensed data to the main CH by several nodes may incur unnecessary communication overhead. Fig. 11(b) depicts several nodes sensing an area with matching FoVs while facing different directions. Consider SC-2 (comprised of audio nodes), which has nodes recording intruder audio when an object enters the vicinity. Following the naive approach, each sensor node initiates its transmission towards the main CH in its respective time slot, which may result in useless transmissions caused by nodes capturing identical data.

- c. **Nodes with differing FoVs facing different directions:** Fig. 11(c) illustrates these nodes, which may each capture unique information due to their deployment. The use case scenario of this sort of deployment is as follows:

In WSNs, nodes are deployed in a field of interest to detect application-specific targets. It is highly likely that every node in the SC faces a different direction with a different FoV. Therefore, transmitting data from a single potential node in the SC can result in data loss.

Suppose six multimedia nodes (i.e., M1, M2, M3, M4, M5, and M6) are randomly deployed in a sensor field, as shown in Fig. 11(c). When an intrusion takes place, a single node may capture the target, while other nodes may not capture due to their different facing directions. To avoid data loss and uphold application integrity, all nodes forward their captured data to the SCH, and the SCH forwards the miniaturized intruder information to the main CH node.

d. **Overlapping nodes:** Consider a scenario where the FoVs of several sensor nodes overlap, as shown in Fig. 11(d). To compute the overlapping FoV, we employ the procedure provided by Ref. [33]. Suppose an intruder (with a weapon) enters a sensitive zone from the south and moves northward. The information captured by each node may or may not be identical (e.g., the intruder's pose captured by a north-facing node may differ from a south-facing node). To avoid this loss, the data captured by both nodes must be considered. Therefore, PE-WMoT allows the SCH to collect data from its SC nodes and remove redundancies (if any) to uphold application QoS.

5. Performance evaluation

5.1. Performance evaluation metrics

We performed several experiments to evaluate the performance of both our PE-WMoT protocol and the benchmark protocol of Evolutionary-Game-based Routing (EGR) [31]. The performance metrics considered include: 1) total energy consumption, 2) Packet Delivery Ratio (PDR), 3) control overhead, 4) CH lifetime, and 5) the impact of overlapping FoVs. These metrics are defined as follows.

The *CH lifetime* denotes the amount of time a node can perform its duties as a CH.

PDR represents the total number of packets successfully delivered at the CH to the total number of packets sent:

$$PDR = \frac{\text{Total Number of Packets Received}}{\text{Total Number of Packets Sent}} \tag{12}$$

The energy consumption of a WSN node mainly depends on packet transmissions, receptions, and processing. The cumulative energy consumption of a single node is:

$$E_{node} = E_{proc} + E_{rx} + E_{tx} \tag{13}$$

Therefore, the *total energy consumption* of the network is:

$$E_{network} = \sum_{i=1}^n (E_{node_i}) \tag{14}$$

where *n* denotes the total number of nodes in the network.

The *control overhead* refers to the number of control packets (e.g., HELLO message, CH announcement packets, Join-CH packets, and TDMA packets) generated to establish the route between a source node and a destination node (e.g., SCH, CH, sink).

We also analyzed the performance of PE-WMoT in terms of packet transmissions and energy consumption by considering directionally overlapping FoVs. The proportion of overlapping FoVs was varied, and the number of transmissions (as well as their effect on node energy consumption) was analyzed.

5.2. Simulation environment

We selected EGR for comparison, as it is closely related to our proposed scheme and the most recent work in the literature. EGR achieves energy efficiency and mitigates the redundant transmissions by computing the overlapping FoVs. It also adopts a game theory approach to electing its CHs.

Simulations were performed in a Castalia simulator [35] (based on OMNET++) developed to simulate a network of low power devices (i.e., WSNs). In the simulations, we used a random topology composed of 105 heterogeneous multimedia nodes randomly deployed in a 100 m × 100 m

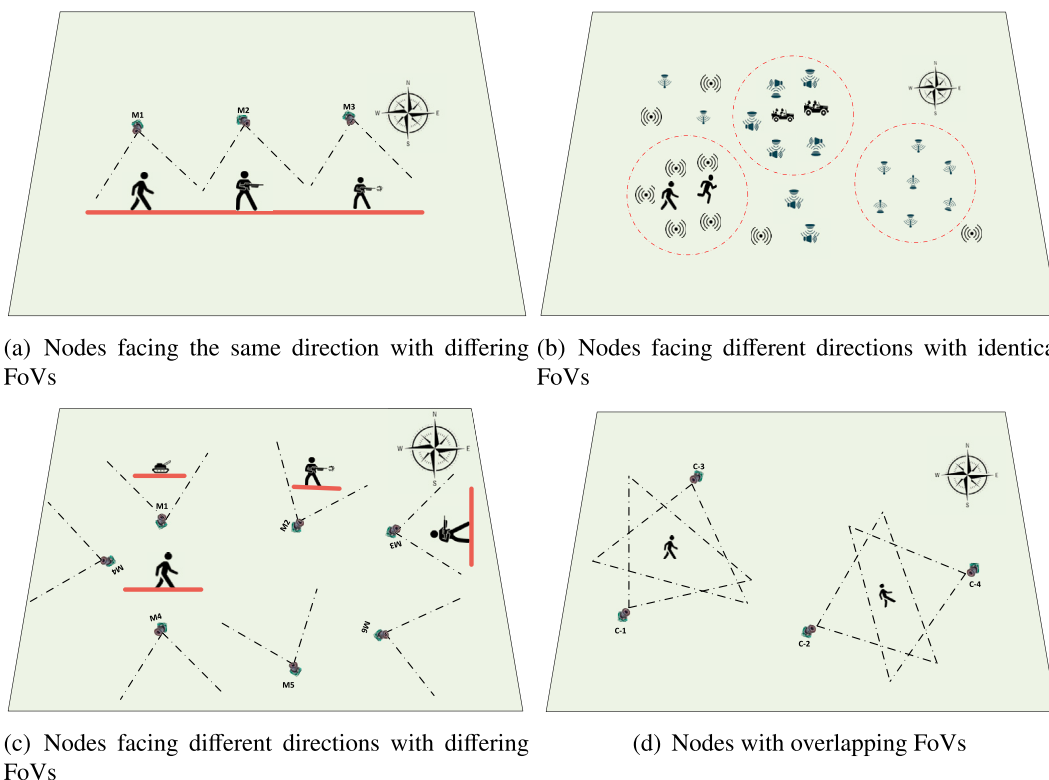


Fig. 11. Traffic generation based on directional FoVs.

area. It is assumed that, among these nodes, CH nodes are rich in terms of available resources while child nodes are resource-constrained. The percentage of CH nodes is 5 %. Under the administration of each cluster, the SCH percentage is 20 %. The initial energy of the nodes varied from 6 to 10 J, while the per bit energy consumption was 0.5 μ J. The rationale is that, in general, the workload of CH is an order of magnitude higher than that of the child nodes. Moreover, the maximum data storage capacity of each CH node was 2^{24} bits. All deployed nodes were equipped with GPS as well as digital compass modules. The simulations were performed for 10,000 s. Each experiment was conducted five times, and the acquired results were the averaged values of the measurements. The major simulation parameters are depicted in Table 7.

5.3. Results and discussion

5.3.1. CH lifetime

The outcomes of the CH lifetime testing for both protocols are presented in Fig. 12. We investigated the CH lifetime of both schemes by varying the number of nodes as well as the packet rates in the network. The results revealed that the PE-WMoT protocol provided a significantly higher CH lifetime than EGR.

This longer CH lifetime mainly depends on the residual energy accompanied by the computational capability and available storage of the node. As PE-WMoT only assigns CH duties to high-resource nodes, this minimizes frequent reclustering chances that may arise due to a lack of available resources. By contrast, EGR only assigns CH duties to high energy nodes. Therefore, in traffic-intensive conditions, CH nodes are unable to accommodate incoming packets from child nodes due to storage and computational capability deficiencies, increasing congestion and re-transmissions in the network.

The proposed subclustering mechanism also minimized the number of dispensable data transmissions. The SCH aggregated data from its SC member nodes, performed data filtration, and transmitted miniaturized data to the main CH. By doing so, it reduced frequent transmissions and excessive CH computations to improve CH lifetime.

The EGR protocol saw CHs consume a high proportion of energy in handling redundant transmissions, lowering overall CH lifetime.

5.3.2. Packet delivery ratio

Fig. 13 visualizes the PDR as a function of the number of network nodes. As discussed, the PE-WMoT protocol directed child nodes to forward their data to their corresponding SCH, and each SCH performed data filtration before forwarding the data to the main CH. Therefore, the PDR was calculated at both the SCH and CH to obtain averaged results.

The results illustrate that the PE-WMoT protocol outperformed the EGR protocol in terms of PDR. The rationale is that due to high available resources, each CH accommodated more incoming packets from its subordinate SCHs. Furthermore, the proposed efficient subclustering mechanism highly mitigated the number of useless packet transmissions. In addition, storage and computation capacity considerations (in conjunction with energy available during CH and SCH selection) enabled increased data packet handling from underlying nodes.

In EGR, the identical data transmissions, lack of consideration regarding available storage, and computational capability exhausted each CH. This prevented each CH from accommodating incoming packets from SCHs, caused packet drop rates to increase, and reduced PDR.

5.3.3. Total energy consumption

Fig. 14 shows the total energy consumption as a function of the number of nodes in the network. The results show that the PE-WMoT protocol achieved remarkably lower energy consumption (approximately 40 %) than the EGR protocol in all nodes densities. This was due to a high amount of available resources enabling CHs to perform their duties for long periods of time, minimizing control overhead and packet

Table 7
Simulation parameters.

Parameters	Values
Simulator	Castalia
Area	100 m \times 100 m
Number of nodes	105
Node distribution	Random
Per bit energy consumption	0.5 μ J
Percentage of CH nodes	5 %
Percentage of SCH nodes	20 %
Initial energy of nodes	6–10J
Data packet rate	5 and 10 pkts/sec
Data packet size	128 bytes
Max buffer size	Max 2^{24} bits
Physical layer	IEEE 802.15.4
Simulation time	10,000 s

retransmission.

In addition, the proposed subclustering mechanism diminished undesirable packet transmissions to the main CH by organizing identical application base nodes into subclusters. The child nodes transmitted their sensed data to their respective SCHs positioned at a shorter distance. The shorter-distant transmissions highly minimized the energy consumption of the child nodes. In addition, the transmission of the filtered data significantly reduced the traffic load on the CH. However, the EGR protocol only considered nodes with overlapping FoVs during the data transmission process; therefore, if several nodes had overlapping FoVs, only one was selected to transmit data. It is probable that only a small proportion of nodes may have overlapping FoVs. In such cases, nodes with non-overlapping FoVs transmitted their data directly.

In our simulation settings for EGR, only 40 % of nodes had overlapping FoVs. A significant percentage of non-overlapping nodes transmitted their data to the main CH node without considering the same application type nodes in their close vicinity. The redundant (i.e., similar) data transmissions caused network congestion, frequent retransmissions, and increased.

5.3.4. Control overhead

It is evident from the results depicted in Fig. 15 that the EGR protocol underperformed in comparison with the PE-WMoT protocol in terms of control packet overhead. As expected, the control overhead of the PE-WMoT protocol was low compared to the EGR protocol. Since the control packet transmissions were highly correlated with frequent

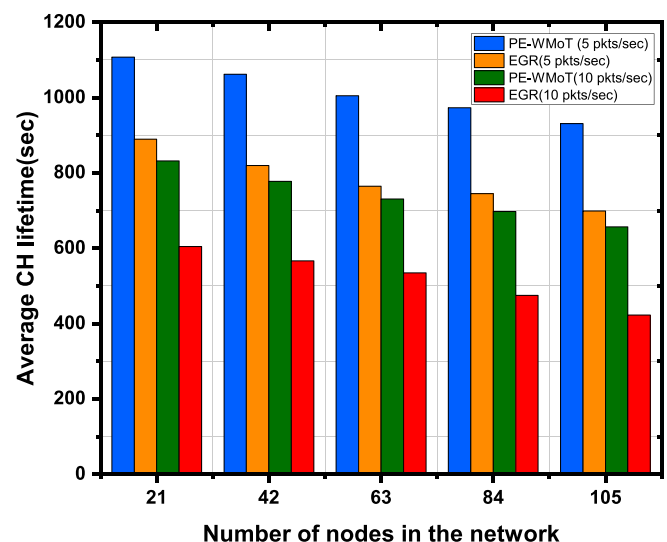


Fig. 12. Average CH lifetime.

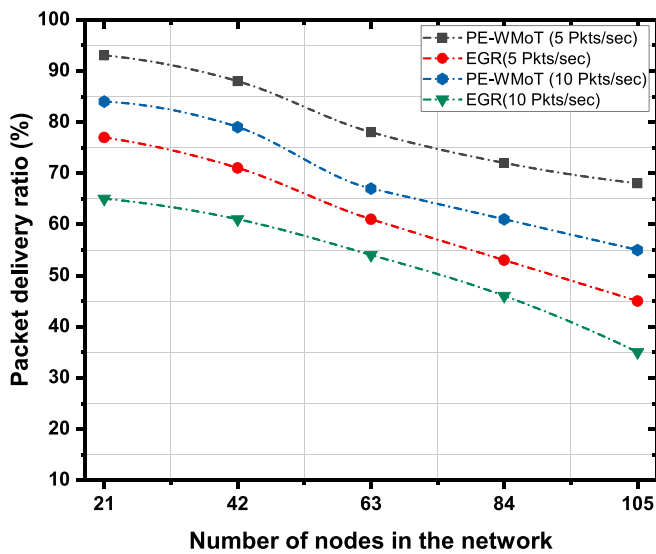


Fig. 13. Packet delivery ratio.

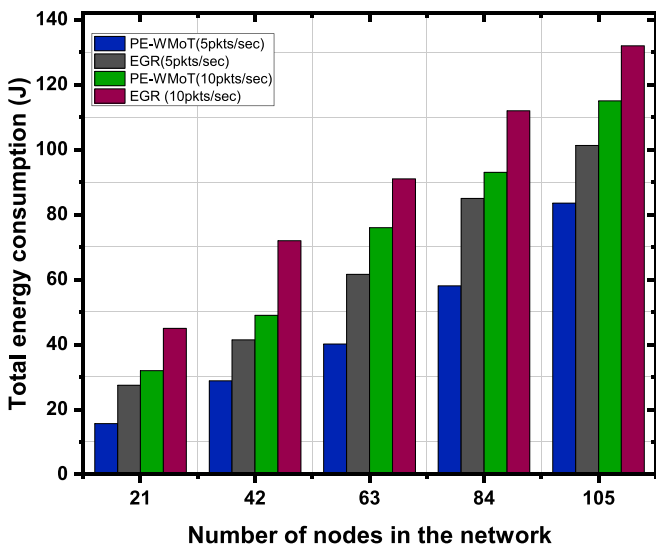


Fig. 14. Total energy consumption.

reclustering, the PE-WMoT protocol significantly reduced reclustering frequency. Moreover, in the PE-WMoT protocol, only a single high energy node shared its neighbors’ information with the CH during the association phase, reducing the number of association packets. Furthermore, the subclustering mechanism of PE-WMoT protocol lowered excessive network transmissions. The CH selection and subclustering mechanism led to an increased CH lifetime and reduced control overhead.

5.3.5. The impact of overlapping FoVs

In addition to the aforementioned performance analyses, we also analyzed the number of transmissions in the proposed work and compared it to the EGR protocol by varying the proportion of nodes along with the overlapping FoV ratio. To carry out these experiments, we introduced parameter β to denote the ratio of overlapping FoVs of various network nodes. Fig. 16 illustrates the total number of data transmissions as well as the total energy consumption of the network at different values of β . We varied the percentage of overlapping nodes between 25 % and

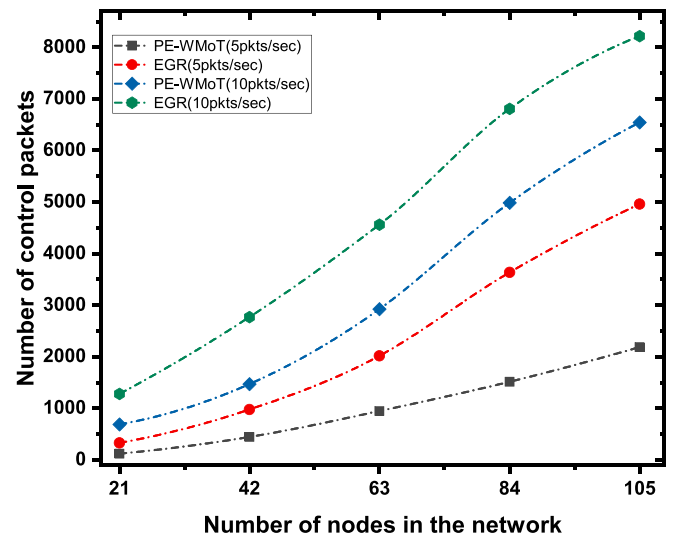


Fig. 15. Number of control packets transmissions in the network.

75 %. Comparing the results depicted in Fig. 16, it is clear that the network consumed more energy due to excessive transmission amounts when there were fewer overlapping nodes.

As the ratio of overlapping nodes increased, the number of transmissions decreased, causing an overall drop in energy consumption. However, despite having a low fraction of overlapping FoVs, the PE-WMoT protocol reduced the number of transmissions (shown in Fig. 16(a)) as well as the total energy consumption in the network (shown in Fig. 16(c)) by employing the subclustering mechanism.

The sub-clustering allowed closely located same-application nodes to transmit their sensed data to SCH residing at a shorter distance from them. These shorter distance transmissions helped nodes conserve energy compared to those that transmitted directly to the main CH. Furthermore, the data aggregation and data filtration at the SCH played a vital role in reducing the number of data transmissions, reducing the load of the main CH node.

In EGR, the number of transmissions to the CH increased as the number of overlapping regions decreased since EGR only considers overlapping nodes for mitigating nonessential transmissions. However, due to the low percentage of overlapping nodes, the number of transmitting nodes increased, which increased the number of transmissions (shown in Fig. 16(b)). Therefore, the total energy consumption of the network also increased, as depicted in Fig. 16(d).

6. Conclusion

In this paper, we proposed a PE-WMoT protocol that would prevent redundant packet transmissions, reduce node energy consumption, and maximize the network operation period. In this regard, a robust sub-clustering strategy was formulated, and SCHs were selected for each SC. The member nodes from each SC forwarded captured data towards their respective SCH, which performed data aggregation and transmitted filtered data to the main CH in order to prevent network congestion. Furthermore, the consideration of available resources during the CH declaration process enabled CHs to accommodate more subordinate (e.g., SCH) traffic. The proposed procedure effectively decreased packet retransmission frequency caused by buffer overflow during abnormal traffic conditions. To prevent data loss and ensure received data quality, the PE-WMoT protocol employed different transmission scenarios based on the directional and overlapped FoVs of deployed nodes. Overall, the simulation results proved that our PE-WMoT protocol outperformed the EGR protocol in terms of energy consumption, packet delivery ratio, control overhead, and CH lifetime.

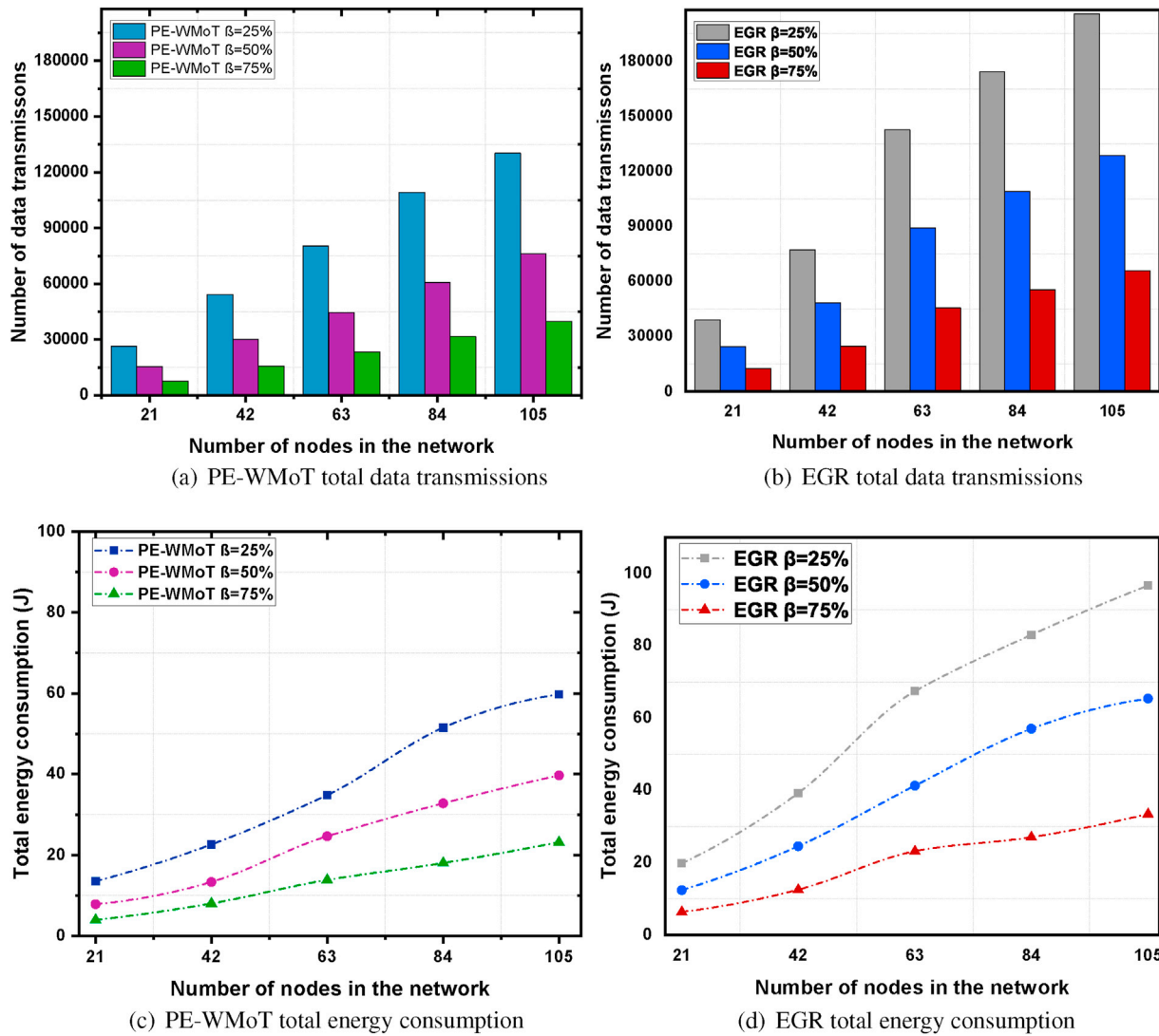


Fig. 16. The impact of overlapping FoVs network energy consumption.

Declaration of competing interest

The authors declare that there is no conflict of interest regarding the publication of this paper.

Acknowledgements

This work was supported in part by the Institute of Information & communications Technology Planning & Evaluation (IITP) grant funded by the Korea government (MSIT) (No.2018-0-01411, A Micro-Service IoTWare Framework Technology Development for Ultra small IoT Device) and in part by 2021 Hongik University Innovation Support program Fund.

References

[1] S.A. Nandhini, R. Hemalatha, S. Radha, K. Indumathi, Web enabled plant disease detection system for agricultural applications using wmsn, *Wireless Pers. Commun.* 102 (2) (2018) 725–740.
 [2] M.A.U. Rehman, R. Ullah, B.-S. Kim, B. Nour, S. Mastorakis, Cdic-wsn: an architecture for single channel cluster-based information-centric wireless sensor networks, *IEEE Int. Things J.* (2020) 1, <https://doi.org/10.1109/JIOT.2020.3041096>.
 [3] M. S. u. din, M. A. U. Rehman, R. Ullah, C.-W. Park, B. S. Kim, Towards network lifetime enhancement of resource constrained iot devices in heterogeneous wireless

sensor networks, *Sensors* 20 (15). doi:10.3390/s20154156. URL <https://www.mdpi.com/1424-8220/20/15/4156>.
 [4] M.A. Ur Rehman, R. Ullah, B.-S. Kim, A compact ndn architecture for cluster based information centric wireless sensor networks, in: *Proceedings of the 6th ACM Conference on Information-Centric Networking, ICN '19*, Association for Computing Machinery, New York, NY, USA, 2019, pp. 163–164, <https://doi.org/10.1145/3357150.3357415>, 10.1145/3357150.3357415. URL.
 [5] M.S.u. din, M.A.U. Rehman, B.-S. Kim, Cidf-wsn: a collaborative interest and data forwarding strategy for named data wireless sensor networks, *Sensors* 21 (15) (2021), 5174, <https://doi.org/10.3390/s21155174>, 10.3390/s21155174. URL.
 [6] A. Boulmaiz, D. Messadeg, N. Doghmane, A. Taleb-Ahmed, Robust acoustic bird recognition for habitat monitoring with wireless sensor networks, *Int. J. Speech Technol.* 19 (3) (2016) 631–645.
 [7] X. Fu, G. Fortino, P. Pace, G. Aloï, W. Li, Environment-fusion multipath routing protocol for wireless sensor networks, *Inf. Fusion* 53 (2020) 4–19, <https://doi.org/10.1016/j.inffus.2019.06.001>. URL, <http://www.sciencedirect.com/science/article/pii/S1566253519301654>.
 [8] A. Ukil, S. Bandyopadhyay, C. Puri, A. Pal, Iot healthcare analytics: the importance of anomaly detection, in: *2016 IEEE 30th International Conference on Advanced Information Networking and Applications (AINA)*, IEEE, 2016, pp. 994–997.
 [9] R. Ullah, M. A. U. Rehman, B. S. Kim, Hierarchical name-based mechanism for push-data broadcast control in information-centric multihop wireless networks, *Sensors* 19 (14). doi:10.3390/s19143034. URL <https://www.mdpi.com/1424-8220/19/14/3034>.
 [10] M. A. U. Rehman, R. Ullah, B. S. Kim, Ninq: Name-integrated query framework for named-data networking of things, *Sensors* 19 (13). doi:10.3390/s19132906. URL <https://www.mdpi.com/1424-8220/19/13/2906>.
 [11] M. Srbínovska, C. Gavrovski, V. Dimcev, A. Krkoleva, V. Borozan, Environmental parameters monitoring in precision agriculture using wireless sensor networks, *J. Clean. Prod.* 88 (2015) 297–307.

- [12] M.Z. Hasan, H. Al-Rizzo, F. Al-Turjman, A survey on multipath routing protocols for qos assurances in real-time wireless multimedia sensor networks, *IEEE Commun. Surv. Tutorials* 19 (3) (2017) 1424–1456, <https://doi.org/10.1109/COMST.2017.2661201>.
- [13] A. A. Abba Ari, A. C. Djedouboum, A. M. Gueroui, O. Thiare, A. Mohamadou, Z. Aliouat, A three-tier architecture of large-scale wireless sensor networks for big data collection, *Appl. Sci.* 10 (15). doi:10.3390/app10155382. URL <https://www.mdpi.com/2076-3417/10/15/5382>.
- [14] Y. Yang, M.I. Fonoage, M. Cardei, Improving network lifetime with mobile wireless sensor networks, *Comput. Commun.* 33 (4) (2010) 409–419, <https://doi.org/10.1016/j.comcom.2009.11.010>. URL <http://www.sciencedirect.com/science/article/pii/S0140366409002990>.
- [15] I.T. Almalkawi, M. Guerrero Zapata, J.N. Al-Karaki, J. Morillo-Pozo, Wireless multimedia sensor networks: current trends and future directions, *Sensors* 10 (7) (2010) 6662–6717.
- [16] Y. Li, Y. Liang, Q. Liu, H. Wang, Resources allocation in multicell d2d communications for internet of things, *IEEE Int. Things J.* 5 (5) (2018) 4100–4108, <https://doi.org/10.1109/JIOT.2018.2870614>.
- [17] T.M. Behera, S.K. Mohapatra, U.C. Samal, M.S. Khan, M. Daneshmand, A.H. Gandomi, Residual energy-based cluster-head selection in wsn for iot application, *IEEE Int. Things J.* 6 (2019) 5132–5139, <https://doi.org/10.1109/JIOT.2019.2897119>.
- [18] Y. Li, J. Liu, B. Cao, C. Wang, Joint optimization of radio and virtual machine resources with uncertain user demands in mobile cloud computing, *IEEE Trans. Multimed.* 20 (9) (2018) 2427–2438, <https://doi.org/10.1109/TMM.2018.2796246>.
- [19] X. Huang, Y. Cui, Q. Chen, J. Zhang, Joint task offloading and qos-aware resource allocation in fog-enabled internet-of-things networks, *IEEE Int. Things J.* 7 (8) (2020) 7194–7206, <https://doi.org/10.1109/JIOT.2020.2982670>.
- [20] J. Wang, Y. Zhang, J. Wang, Y. Ma, M. Chen, Pwdgr: pair-wise directional geographical routing based on wireless sensor network, *IEEE Int. Things J.* 2 (1) (2015) 14–22, <https://doi.org/10.1109/JIOT.2014.2367116>.
- [21] C. Intanagonwiwat, R. Govindan, D. Estrin, J. Heidemann, F. Silva, Directed diffusion for wireless sensor networking, *IEEE/ACM Trans. Netw.* 11 (1) (2003) 2–16.
- [22] K. Shin, J. Song, J. Kim, M. Yu, P.S. Mah, Rear: reliable energy aware routing protocol for wireless sensor networks, in: *The 9th International Conference on Advanced Communication Technology*, vol. 1, 2007, pp. 525–530, <https://doi.org/10.1109/ICACT.2007.358410>.
- [23] Y. Sun, H. Ma, L. Liu, et al., Asar: an ant-based service-aware routing algorithm for multimedia sensor networks, *Front. Electr. Electron. Eng. China* 3 (1) (2008) 25–33.
- [24] E. Sun, X. Shen, H. Chen, A low energy image compression and transmission in wireless multimedia sensor networks, *Procedia Eng.* 15 (2011) 3604–3610.
- [25] Y. Wang, D. Wang, X. Zhang, J. Chen, Y. Li, Energy-efficient image compressive transmission for wireless camera networks, *IEEE Sensor. J.* 16 (10) (2016) 3875–3886.
- [26] Y. Li, S. Xia, Q. Yang, G. Wang, W. Zhang, Lifetime-priority-driven resource allocation for wnv-based internet of things, *IEEE Int. Things J.* 8 (6) (2021) 4514–4525, <https://doi.org/10.1109/JIOT.2020.3029175>.
- [27] H. Oztarak, T. Yilmaz, K. Akkaya, A. Yazici, Efficient and accurate object classification in wireless multimedia sensor networks, in: *2012 21st International Conference on Computer Communications and Networks, ICCCN*, 2012, pp. 1–7, <https://doi.org/10.1109/ICCCN.2012.6289244>.
- [28] N. Magaia, N. Horta, R. Neves, P.R. Pereira, M. Correia, A multi-objective routing algorithm for wireless multimedia sensor networks, *Appl. Soft Comput.* 30 (2015) 104–112.
- [29] C. Li, J. Bai, J. Gu, X. Yan, Y. Luo, Clustering routing based on mixed integer programming for heterogeneous wireless sensor networks, *Ad Hoc Netw.* 72 (2018) 81–90.
- [30] G. Ahmed, J. Zou, M.M.S. Fareed, M. Zeeshan, Sleep-awake energy efficient distributed clustering algorithm for wireless sensor networks, *Comput. Electr. Eng.* 56 (2016) 385–398, <https://doi.org/10.1016/j.compeleceng.2015.11.011>.
- [31] M.A. Habib, S. Moh, Robust evolutionary-game-based routing for wireless multimedia sensor networks, *Sensors* 19 (16) (2019), 3544.
- [32] D. Pescaru, D.-I. Curiaac, Anchor node localization for wireless sensor networks using video and compass information fusion, *Sensors* 14 (3) (2014) 4211–4224.
- [33] M. Alaei, J.M. Barcelo-Ordinas, Node clustering based on overlapping fovs for wireless multimedia sensor networks, in: *2010 IEEE Wireless Communication and Networking Conference, IEEE*, 2010, pp. 1–6.
- [34] R.W. Saaty, The analytic hierarchy process—what it is and how it is used, *Math. Model.* 9 (3–5) (1987) 161–176.
- [35] A. Boulis, Castalia: Revealing Pitfalls in Designing Distributed Algorithms in Wsn, 407–408doi, 2007, <https://doi.org/10.1145/1322263.1322318>, 10.1145/1322263.1322318. URL.